CHARA Field of View in the Lab as Seen by the Star Tracker Camera (STST)

Narsireddy Anugu
2025 Mar 05
A CHARA Technical Report

1. Introduction: Dual-Field Interferometric Mode Concept

In dual-star mode, two beam combiners operate simultaneously, each observing a different object in a double-star system (Fig. 1). One beam combiner collects the flux from the primary star and injects it into a single-mode fiber, while the other captures the companion (Fig. 2), whose separation and position angle relative to the host star are known. The phase-tracking beam combiner focuses on the bright star, measuring its phase with high precision at fast frame rates—on the order of a few milliseconds. This real-time measurement is used to correct for atmospheric disturbances, effectively "freezing" turbulence. As a result, the second beam combiner, which targets the high-contrast companion—potentially an exoplanet—can achieve significantly longer exposure times, often spanning tens of seconds. In this setup, MIRC-X (*Anugu et al. 2020, AJ, 160, 158*) acts as the phase tracker, while MYSTIC (*Setterholm et al. 2023, JATIS, 9, 025006*) serves as the science beam combiner.

Additionally, single-mode fibers serve as spatial filters, removing much of the stellar or non-coherent light and thereby reducing photon noise in the science beam combiner. Furthermore, interferometry with 15 baselines allows for the distinction between flux leakage from the central star and the coherent flux from the companion, as their coherent signals exhibit different phases.

2. Measuring the CHARA Field of View in the Lab

To assess the feasibility of the dual-field interferometric mode at CHARA, we observed eight double stars with separations ranging from 1" to 5" to measure the field of view of CHARA in the lab.

During the S2 drive tests on February 25–26, 2025, we slewed the telescope across several stars, including binary systems, while recording data using the STST (Star Tracker) camera. Image analysis indicated that the CHARA array has a field of view of up to ~5 arcseconds.

Upon comparing the flux ratio of the primary and secondary stars, we initially suspected that the secondary might be vignetted. However, a comparison with data from the WDS catalog suggests that the observed difference is astrophysical in nature rather than an instrumental effect.

3. A Potential Application: Observing the Procyon Binary System

This observing mode opens exciting possibilities, such as testing it on the Procyon binary system to measure the diameter of its white dwarf companion—provided it is large enough to be resolved.

The white dwarf (K~8) is approximately 3000:1 fainter (*Δmag ≈ 9*) than the primary star (K = -1) (*Howard E. Bond et al. 2015, ApJ 813 106*). Procyon, located just 11.46 ± 0.05 light-years away, has a primary-secondary separation of a = 4.3 arcsec, making it an ideal target for such an experiment.

4. Differential Delay Line (DDL) Requirements

To simultaneously obtain fringes on the primary star (with MIRC-X) and the companion (with MYSTIC), the MYSTIC DDLs must move relative to the MIRC-X fringe tracker. The required differential optical path delay (ΔOPD) is given by:

$$\Delta OPD = B \times (S - P)$$

For a binary separation of 1", we need ΔOPD = 1.5 mm (300m × 1").
For a binary separation of 5", we need ΔOPD = 7.5 mm (300m × 5").

Currently, MIRC-X and MYSTIC have 28 mm range DDLs, which should be sufficient if used efficiently. However, if funding allows, upgrading to improved DDLs would enhance resolution and speed.

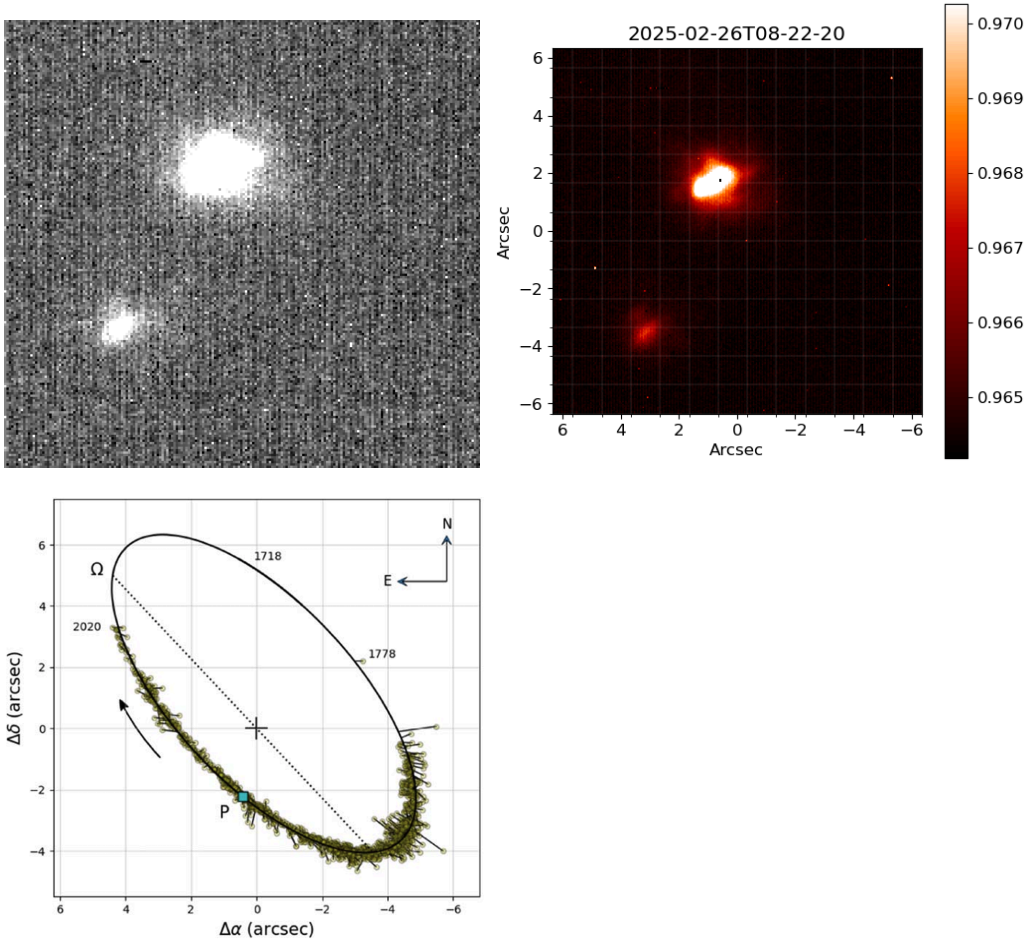

Fig. 1: alf Gem system. (Top left) STST screenshot. (Top right) STST image with scale, showing a binary separation of 5.4 arcseconds. (Bottom left) Torres 2022, ApJ 941:8 (a different epoch; note that comparison is not valid as the STST orientation is not calibrated).

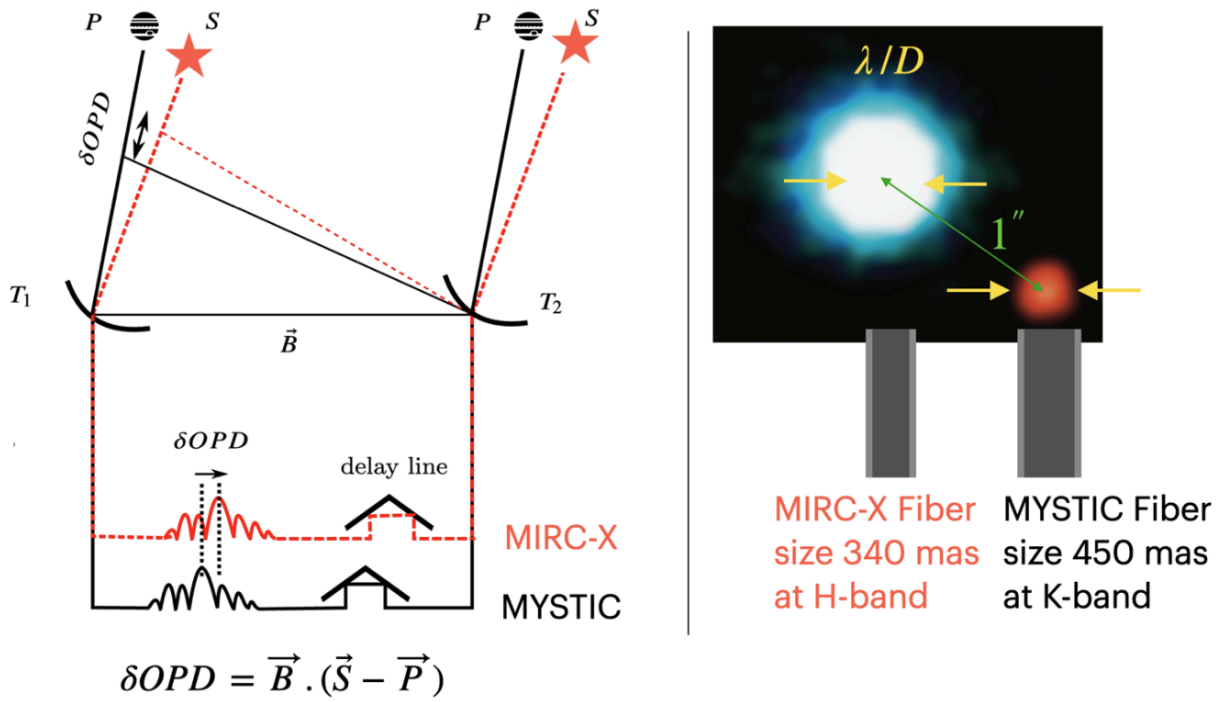

$$\delta OPD = \vec{B} . (\vec{S} - \vec{P})$$

Figure 2: (Left) Schematic of dual-star interferometry in action. The star and its planet are observed simultaneously by the MIRC-X (phase tracker; FT) and MYSTIC (science; SC) beam combiners—one centered on the star, the other on the planet. Both interferometers record fringe patterns, with the relative position of these two fringe patterns (known as the relative optical path difference) linked to the scalar product of the star-planet separation vector (S-P) and the baseline vector (B). (Right) The size of the fiber core is optimized to the diffraction limit of the point spread function (PSF) of the 1-m telescope, which is $\lambda/D = 340$ *mas and 450 mas in H-band and K-bands.*

1. alf Gem, Castor AB (Az=280.9, El=49.5)

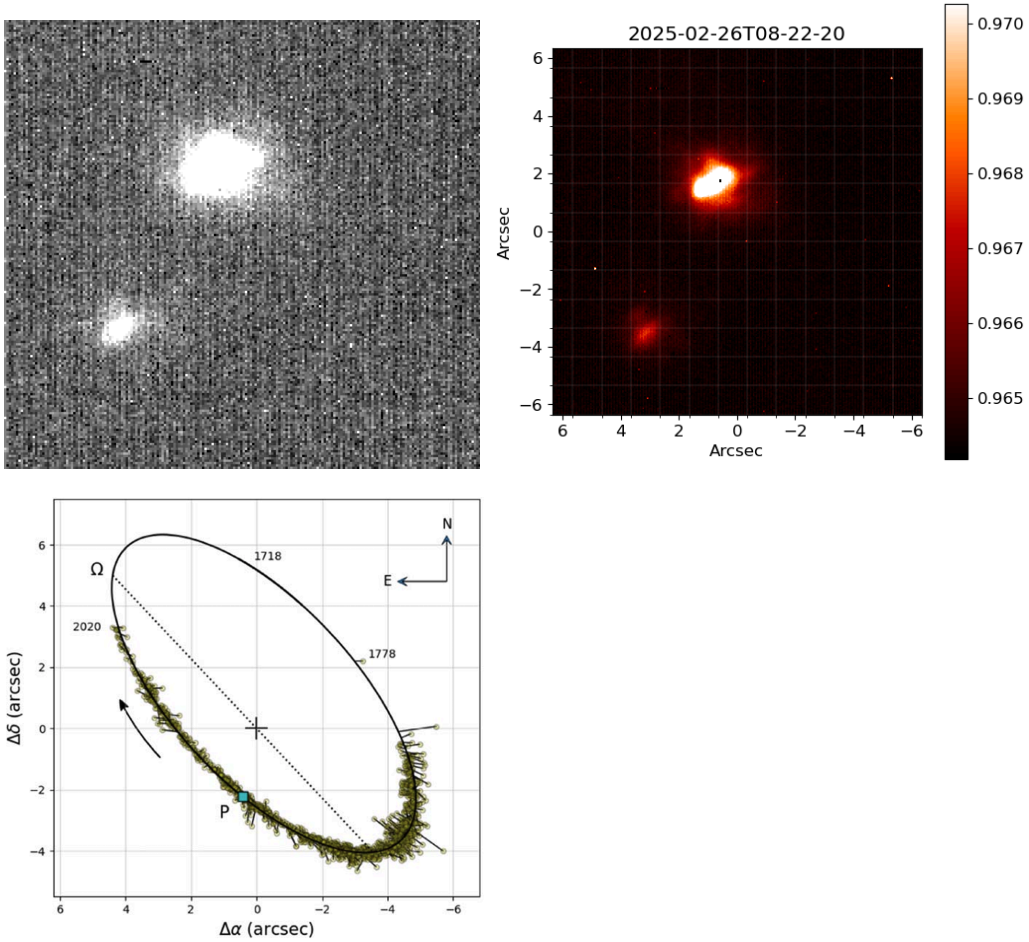

Fig. 1: alf Gem system. (Top left) STST screenshot. (Top right) STST image with scale, showing a binary separation of 5.4 arcseconds. (Bottom left) Torres 2022, ApJ 941:8 (a different epoch; note that comparison is not valid as the STST orientation is not calibrated).

WDS catalog, last epoch 2023,
Sep=5.4 as,
THETA=51,
Mag_pri=1.93,
Mag_Sec=2.97
Torres_2022_ApJ_941_8
https://iopscience.iop.org/article/10.3847/1538-4357/ac9d8d

2. gam Leo (Az=226.8, El=70.2)

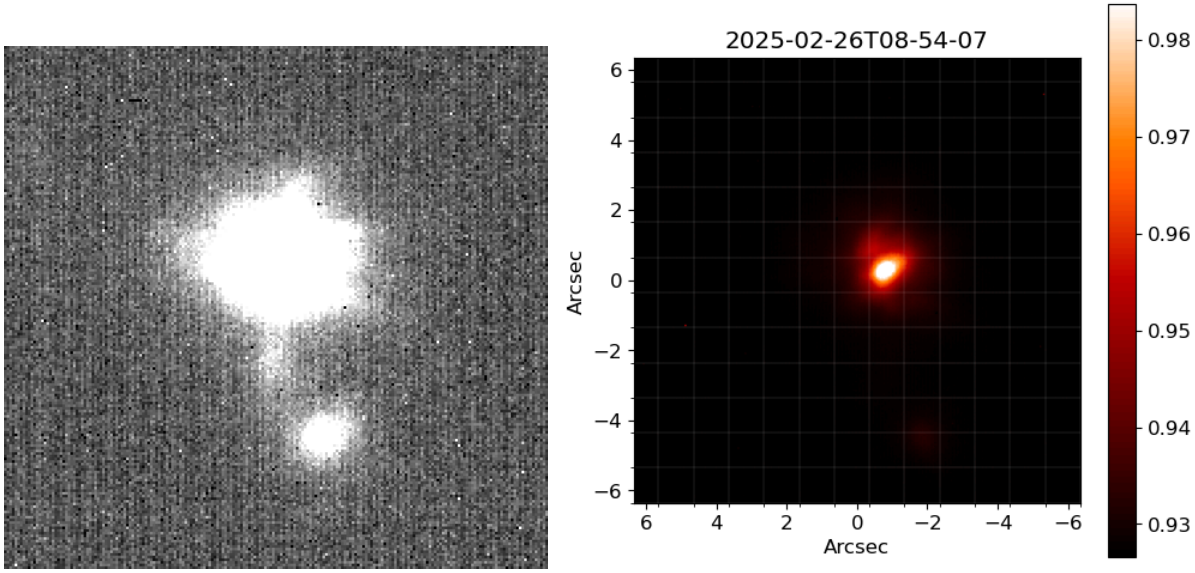

Fig. 2: gam Leo. (Left) STST screenshot. (Right) STST image with scale, showing a binary separation of 4.7 arcsecond.

WDS catalog, last epoch 2022.8
Sep=4.7 as,
THETA=127,
Mag_pri=2.37,
Mag_Sec=3.64
http://stars.astro.illinois.edu/sow/algieba.html

3. Ksi UMa (Az=83.8, El=56.7)

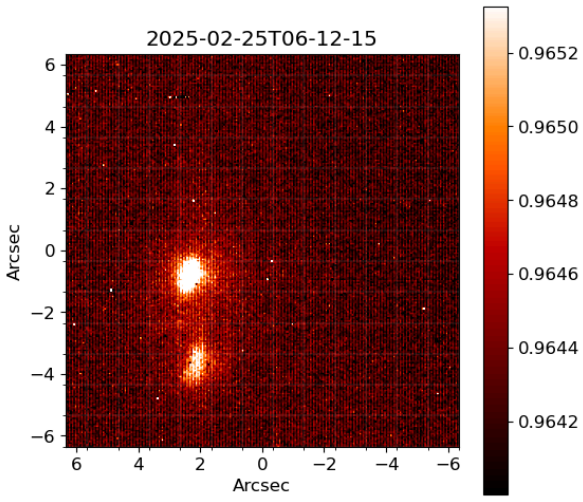

Fig. 3: Ksi UMa. STST image with scale, showing a binary system with a separation of 2.4 arcseconds.

WDS catalog, last epoch 2022.16
Sep=2.4 as,
THETA=144,
Mag_pri=4.33,
Mag_Sec=4.8

4. gam Vir (Az=133.5, El=43.3)

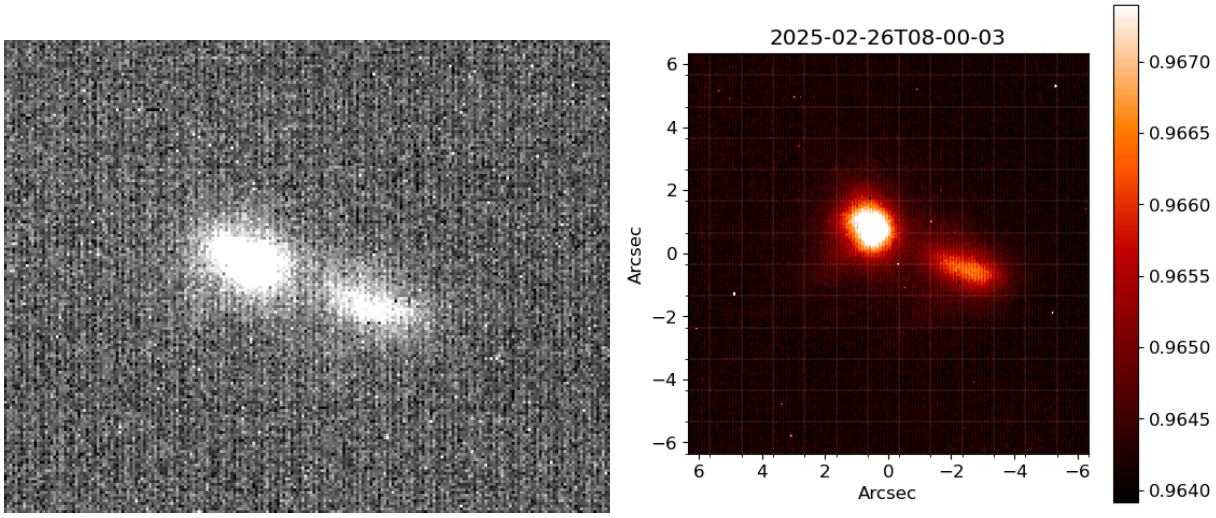

Fig 4: gam Vir. (Left) STST screenshot, (Right) STST image with scale, showing a binary system with a separation of 3.2 arcseconds.

WDS catalog, last epoch 2022.16
Sep=3.2 as,
THETA=354,
Mag_pri=3.48,
Mag_Sec=3.56

5. zet Cnc (Az=196, El=72.8)

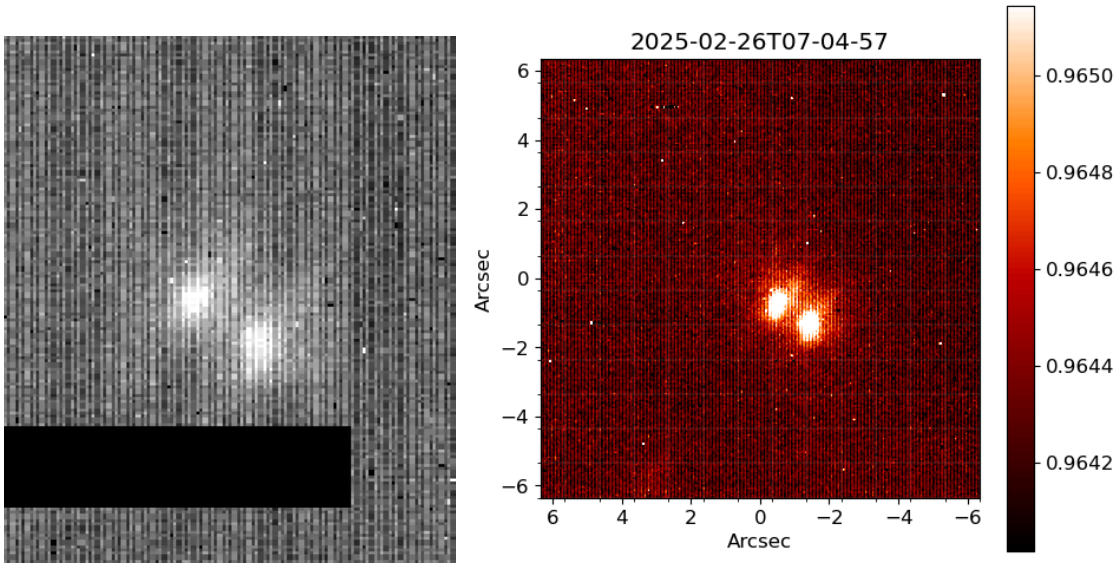

Fig 5: zet Cnc. (Left) STST screenshot, (Right) STST image with scale, showing a binary system with a separation of 1.1 arcseconds.

WDS catalog, last epoch 2022.12
Sep=1.1 as
THETA=177
Mag_pri=5.3
Mag_Sec=6.25

6. 32 Ori (AZ=243.1, El=42.6)

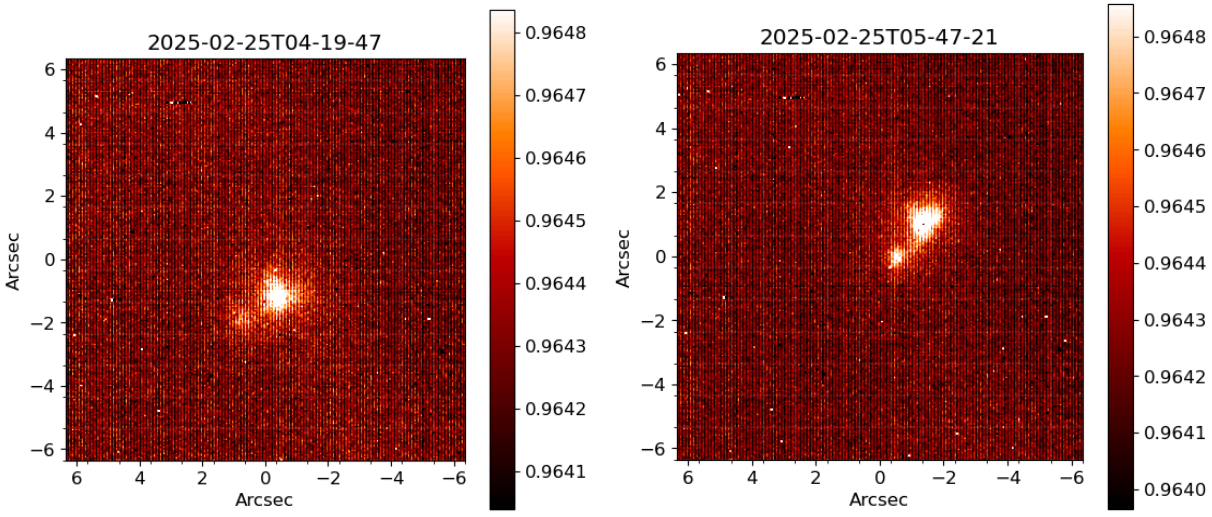

Fig. 6: 32 Ori. (Left and right) STST images showing different slews on February 25, 2025. The binary system has a separation of 1.3 arcseconds.

WDS catalog, last epoch 2022.2
Sep=1.3 as,
THETA=218,
Mag_pri=4.44,
Mag_Sec=5.76

7. Eta Ori (Az=235.2, El=36.9)

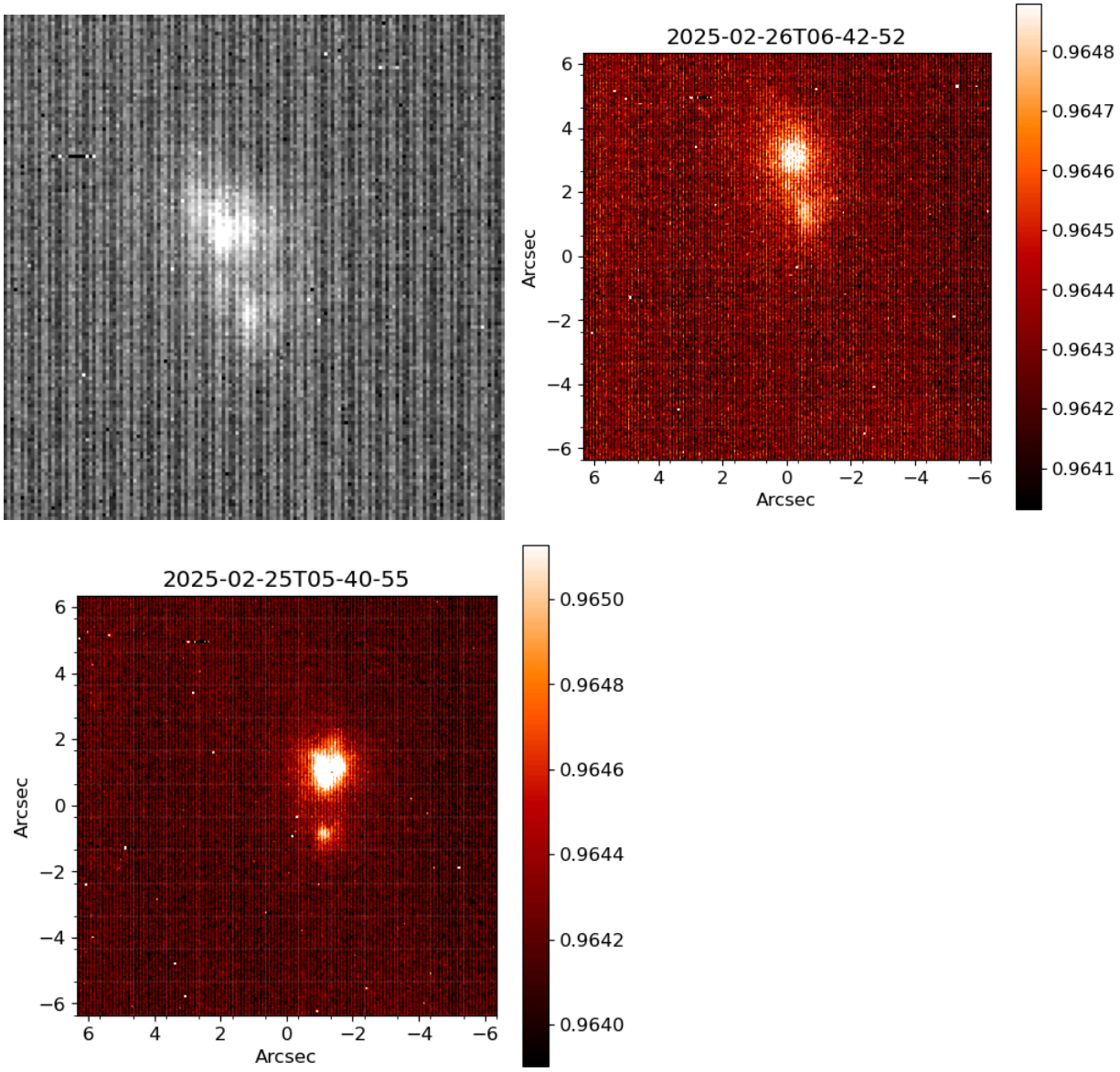

Fig. 7: Eta Ori. (Top left) STST screenshot from February 26, 2025. (Top right) STST image with scale from February 26, 2025, showing the binary system with a separation of 1.8 arcseconds. (Bottom) STST image with scale from February 25, 2025. By comparing the images from the nights of February 25 and 26, we can observe the rotation of the binary system as a result of Earth's rotation.

WDS catalog, last epoch 2023.1
Sep=1.8 as,
THETA=77,
Mag_pri=3.56,
Mag_Sec=4.87

8. 52 Ori (Az=236.4, El=48.2)

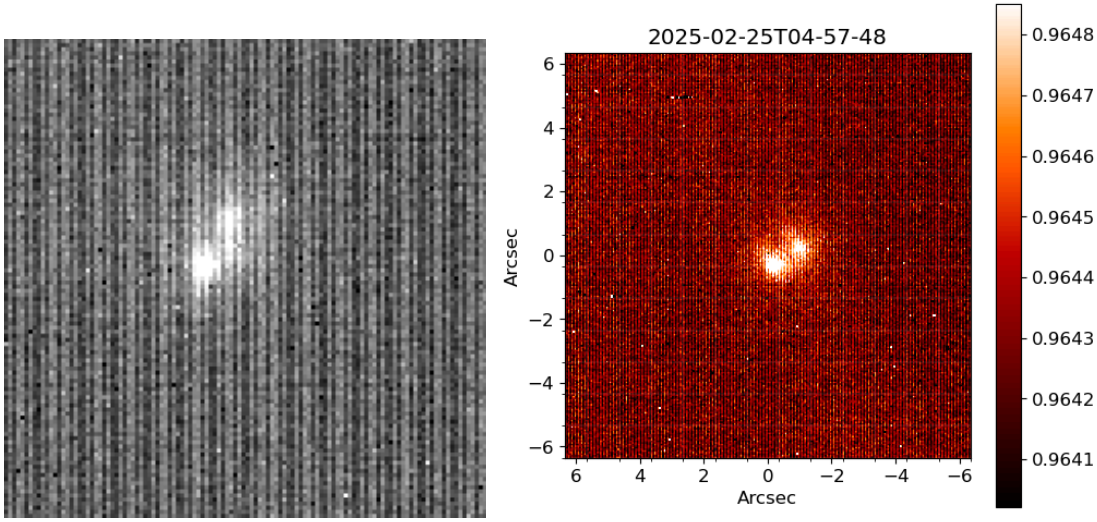

Fig 8: 52 Ori. (Left) STST screenshot, (Right) STST image with scale, showing a binary system with a separation of 1.0 arcseconds.

WDS catalog, last epoch 2022.16
Sep=1.0 as,
THETA=222,
Mag_pri=6.0,
Mag_Sec=6.0